Antibodies to PfSEA-1 block parasite egress from RBCs and protect against malaria infection

Dipak K. Raj *et al.*

Science **344**, 871 (2014);
DOI: 10.1126/science.1254417

RESEARCH ARTICLES

INFECTIOUS DISEASE

Antibodies to PfSEA-1 block parasite egress from RBCs and protect against malaria infection

Dipak K. Raj,[1] Christian P. Nixon,[1] Christina E. Nixon,[1] Jeffrey D. Dvorin,[2] Christen G. DiPetrillo,[2] Sunthorn Pond-Tor,[1] Hai-Wei Wu,[1,3] Grant Jolly,[4] Lauren Pischel,[1] Ailin Lu,[1] Ian C. Michelow,[1,3] Ling Cheng,[1] Solomon Conteh,[5] Emily A. McDonald,[1] Sabrina Absalon,[2] Sarah E. Holte,[6] Jennifer F. Friedman,[1,3] Michal Fried,[5]* Patrick E. Duffy,[5]* Jonathan D. Kurtis[1,4]*†

Novel vaccines are urgently needed to reduce the burden of severe malaria. Using a differential whole-proteome screening method, we identified *Plasmodium falciparum* schizont egress antigen-1 (PfSEA-1), a 244-kilodalton parasite antigen expressed in schizont-infected red blood cells (RBCs). Antibodies to PfSEA-1 decreased parasite replication by arresting schizont rupture, and conditional disruption of PfSEA-1 resulted in a profound parasite replication defect. Vaccination of mice with recombinant *Plasmodium berghei* PbSEA-1 significantly reduced parasitemia and delayed mortality after lethal challenge with the *Plasmodium berghei* strain ANKA. Tanzanian children with antibodies to recombinant PfSEA-1A (rPfSEA-1A) did not experience severe malaria, and Kenyan adolescents and adults with antibodies to rPfSEA-1A had significantly lower parasite densities than individuals without these antibodies. By blocking schizont egress, PfSEA-1 may synergize with other vaccines targeting hepatocyte and RBC invasion.

Plasmodium falciparum malaria is a leading cause of morbidity and mortality in developing countries, infecting hundreds of millions of individuals and killing up to 1 million children in sub-Saharan Africa each year (*1*, *2*). Children suffer the most from malaria, yet vaccine discovery efforts have not targeted this age group. Of the ~100 vaccine candidates currently under investigation, more than 60% are based on only four parasite antigens (*3*, *4*). New antigen candidates are urgently needed, but strategies to identify novel antigens are limited.

Human residents of endemic areas develop protective immunity that limits parasitemia and disease; thus, naturally acquired human immunity provides an attractive model for vaccine antigen identification. Plasma from some chronically exposed individuals contains antibodies that restrict parasite growth ex vivo (*5*) and after adoptive transfer (*6*). One approach to identifying vaccine antigens is to identify malarial proteins that are only recognized by antibodies in the plasma of chronically exposed individuals who remain resistant to infection but are not recognized by antibodies in the plasma of susceptible individuals.

[1]Center for International Health Research, Rhode Island Hospital, The Warren Alpert Medical School of Brown University, Providence, RI 02903, USA. [2]Division of Infectious Diseases, Boston Children's Hospital and Harvard Medical School, Boston, MA 02115, USA. [3]Department of Pediatrics, Rhode Island Hospital, The Warren Alpert Medical School of Brown University, Providence, RI 02903, USA. [4]Department of Pathology and Laboratory Medicine, Rhode Island Hospital, The Warren Alpert Medical School of Brown University, Providence, RI 02906, USA. [5]Laboratory of Malaria Immunology and Vaccinology, National Institute of Allergy and Infectious Diseases, National Institutes of Health, Rockville, MD 20892, USA. [6]Fred Hutchinson Cancer Research Center Program in Biostatistics and Biomathematics, Department of Biostatistics and Global Health, University of Washington, Seattle, WA 98109, USA. *These authors contributed equally to this work. †Corresponding author. E-mail: jonathan_kurtis@brown.edu

Identification and in Silico Evaluation of Vaccine Candidates

Using our cDNA library–based differential screening method (*7*) and plasma and epidemiologic data from a Tanzanian birth cohort (*8*), we probed the *P. falciparum* blood-stage proteome with plasma from resistant and susceptible 2-year-old children to identify parasite proteins that are the targets of protective antibody responses. We selected 2-year-olds because, in our cohort, resistance to *P. falciparum* parasitemia is first detected at this age (fig. S1).

We selected 12 resistant and 11 susceptible 2-year-old children with partial matching for gender and village of residence, which may be related to resistance (table S1). Resistance was determined based on the mean parasite density in all blood films collected from children between ages 2 and 3.5 years. We pooled plasma collected at age 2 years (±2 weeks) from the resistant individuals and the susceptible individuals and performed differential screening experiments on a *P. falciparum* 3D7 strain blood-stage cDNA library. We screened 1.25×10^6 clones and identified three clones that were recognized by antibodies in plasma from resistant, but not susceptible, individuals. The sequences of these clones were compared with the published *P. falciparum* genome (www.PlasmoDB.org) and found to encode nucleotides (nt) 2431 to 3249 of *PF3D7_1021800*, a hypothetical gene on chromosome 10; nt 3490 to 5412 of *PF3D7_1134300*, a hypothetical gene on chromosome 11; and nt 201 to 1052 of *PF3D7_1335100*, which encodes merozoite surface protein-7 (MSP-7), a protein involved in red blood cell (RBC) invasion, which is currently under study as a potential vaccine candidate (*9*–*12*).

In silico analysis (www.PlasmoDB.org and www.OrthoMCL.org) predicted that *PF3D7_1021800* contains a 6744–base pair (bp) gene that encodes a 244-kD acidic phosphoprotein (*13*), with three introns near its 3′ end, and syntenic orthologs in all rodent and primate malarias evaluated to date, but not in other genera. Based on in vitro experiments, we designated the protein product of *PF3D7_1021800* as *Plasmodium falciparum* schizont egress antigen-1 (PfSEA-1) and its corresponding gene as *PfSEA1*. PfSEA-1 contains multiple complex repeat regions and extensive regions of low amino acid complexity, with 50% of the protein being composed of four amino acids (Asn, Lys, Glu, and Asp).

PfSEA1 expression increases throughout blood-stage schizogeny, and the gene displays minimal sequence variation in the immunorelevant region recognized in our differential screens (nt 2431 to 3249). A recently reported deep sequencing effort on 227 field samples identified only three nonsynonymous and one synonymous single-nucleotide polymorphisms in the cloned region (*14*).

Conditional Destabilization of PfSEA-1

PfSEA-1 has no significant homology to proteins of known function. Multiple attempts to disrupt *PfSEA1* by homologous recombination were unsuccessful, which suggests that PfSEA-1 is essential for blood-stage replication. Using the conditional destabilization (knockdown) system, we generated a parasite strain with a destabilization domain and hemagglutinin (HA) tag fused to the C terminus of endogenous PfSEA-1 (*15*) and verified the strain by Southern blot and sequencing across the insertion boundary (fig. S2, A and B). After removal of the stabilizing agent, Shield-1, expression of PfSEA-1 decreased by 75% (Fig. 1A), and parasites with destabilized expression of PfSEA-1 had a marked, 80% inhibition of parasite replication as compared with parasites expressing normal levels of PfSEA-1 (Fig. 1B). In addition, parasites grown for a single cycle in the absence of Shield-1 had delayed schizont egress (fig. S2C) accompanied by a 40% decrease in the number of ring-stage parasites 12 hours after schizont rupture (fig. S2D). The addition of Shield-1 did not alter the replication of wild-type parasites (fig. S3), and conditional destabilization of nonessential genes did not produce a replication defect (*15*, *16*).

Expression and Validation of rPfSEA-1

We expressed and purified the polypeptide encoded by the differentially recognized immunorelevant

region (nt 2431 to 3249, amino acids 810 to 1083) in *Escherichia coli* and designated this recombinant protein rPfSEA-1A (fig. S4A). Before evaluation in the entire birth cohort, we performed an initial validation enzyme-linked immunosorbent assay (ELISA) using an independent selection of resistant and susceptible individuals from our Tanzanian birth cohort (table S2). Immunoglobulin G (IgG) antibody recognition of rSEA-1A was 4.4-fold higher in plasma pooled from resistant individuals (n = 11) than in susceptible individuals (n = 14, fig. S4B). This pattern of recognition was not observed for other malaria proteins and controls (fig. S4C), which supported our library screening results.

We have cloned the immunorelevant region into a eukaryotic expression plasmid (VR2001) and immunized mice with either the recombinant protein (rPfSEA-1A) or DNA constructs to generate antisera to PfSEA-1A (anti–PfSEA-1A). To confirm that *PfSEA1* encodes a parasite protein, we probed *P. falciparum* infected and uninfected RBCs with antisera prepared by DNA vaccination. Anti–PfSEA-1A recognized a 244-kD protein in infected but not uninfected RBCs (fig. S5A), and recognized rPfSEA-1A (fig. S5B).

Anti-PfSEA-1 Mediates Growth Inhibition of Parasites in Vitro

We performed growth inhibition assays using anti–rPfSEA-1A prepared by either DNA or recombinant protein immunization (Fig. 2). Parasites were synchronized to the ring stage, cultured to obtain mature trophozoites, and then incubated with anti–rPfSEA-1A or controls for 24 hours, followed by enumeration of newly invaded ring-stage parasites. Anti–rPfSEA-1A generated by DNA plasmid or recombinant protein–based immunization inhibited parasite growth by 58 to 74% across three parasite strains compared with controls (all $P < 0.009$).

We developed monoclonal antibodies (mAbs) in rPfSEA-1A–immunized mice that recognized rPfSEA-1A by ELISA. Some (mAb CF6), but not all (mAb CF3), mAbs mediated up to 75% growth inhibition at a concentration of 250 μg/ml (Fig. 2F), which is substantially lower than the inhibitory concentration of mAb to MSP-1 (*17*). In addition, we purified human polyclonal antibodies to PfSEA-1 from pooled plasma using rPfSEA-1A coupled to Sepharose beads and demonstrated that these human antibodies to PfSEA-1 significantly inhibited parasite growth (fig. S6, A and B).

Stage-Specific Immunolocalization of PfSEA-1

We immunolocalized PfSEA-1 by immunofluorescence confocal microscopy and immunogold

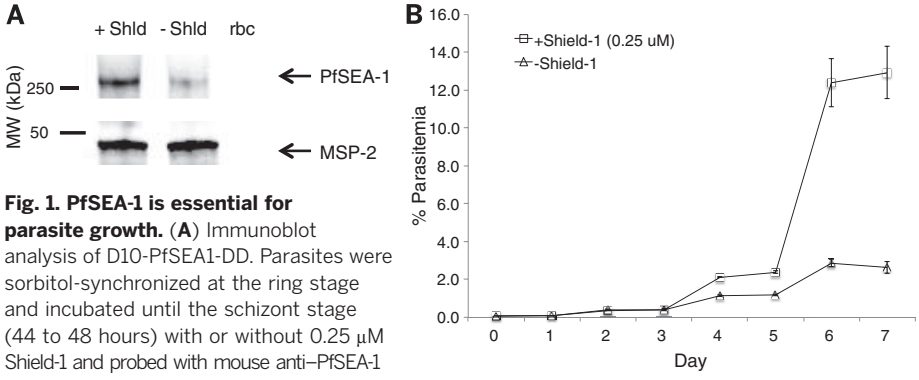

Fig. 1. PfSEA-1 is essential for parasite growth. (**A**) Immunoblot analysis of D10-PfSEA1-DD. Parasites were sorbitol-synchronized at the ring stage and incubated until the schizont stage (44 to 48 hours) with or without 0.25 μM Shield-1 and probed with mouse anti–PfSEA-1 produced by DNA immunization (top panel) or rabbit anti-MSP2 (loading control, bottom panel). Lane 1, Shield-1–treated cultures; lane 2, untreated cultures; lane 3, uninfected RBCs. The top arrow indicates PfSEA-1 fused with a DD tag; the bottom arrow indicates MSP-2. (**B**) Replication curves for D10-PfSEA1-DD parasites. Ring-stage parasites were cultured with or without 0.25 μM Shield-1. Parasitemia was measured by flow cytometry. Each data point represents the mean of three replicates; error bars indicate SEM.

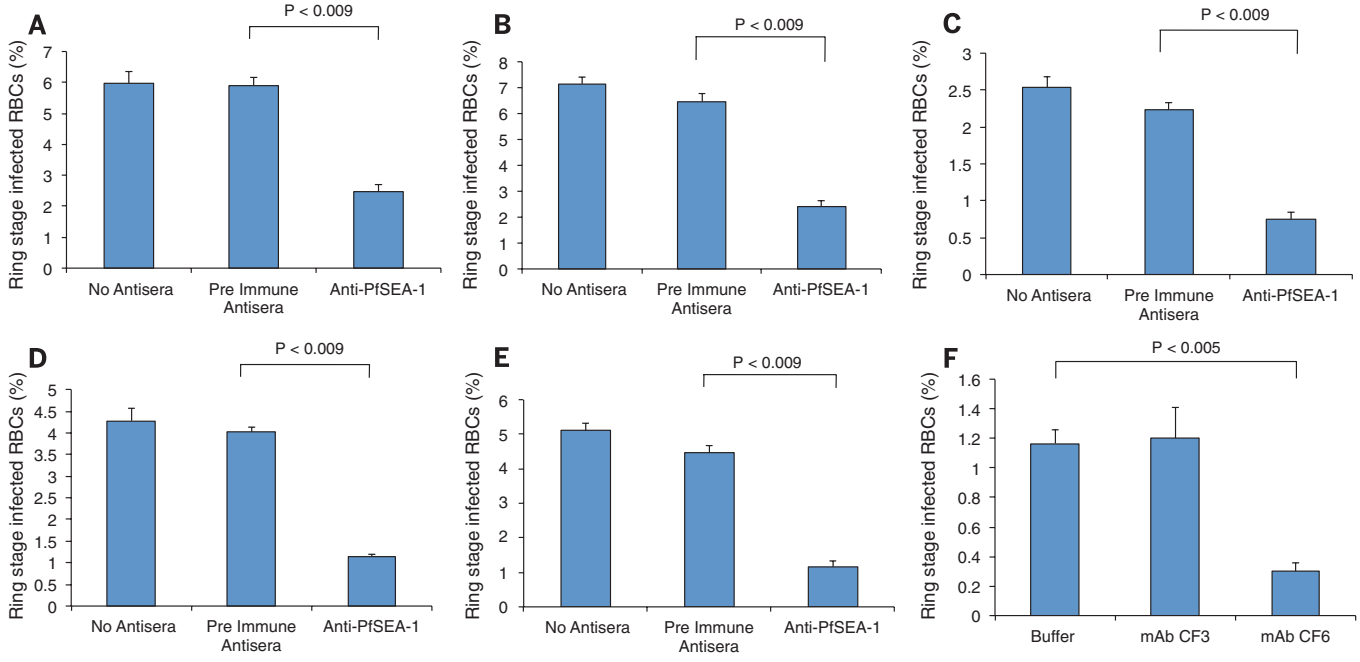

Fig. 2. Antibodies to PfSEA-1 inhibit malaria parasite growth. Polyclonal antibodies to PfSEA-1 generated by DNA (**A** to **C**) and recombinant protein (**D** and **E**) immunization, and mAbs to PfSEA-1 (**F**) inhibit parasite growth and invasion by 58 to 74% for three parasite strains in vitro. Mature trophozoite-stage 3D7 [(A), (D), and (F)], W2 [(B) and (E)], and D10 (C) parasites were were cultured in the presence of mouse antisera to PfSEA-1 [1:10 dilution, (A) to (E)]. Negative controls included no mouse sera and preimmune mouse sera (1:10 dilution). In (F), parasites were incubated in the presence of mAbs to PfSEA-1 CF3 or CF6 (250 μg/ml) or buffer. Parasites were cultured for 24 hours, and ring-stage parasites were enumerated by microscopy. Bars represent the mean of five independent replicates, with each replicate performed in triplicate. Error bars represent SEMs. Comparisons between pre- and postimmune mouse sera by a nonparametric Mann-Whitney U test are indicated. (A) to (C) and (F) are representative of three independent experiments. (D) and (E) are representative of five independent experiments.

transmission electron microscopy (Fig. 3). Anti–PfSEA-1 did not bind to free merozoites, rings, or late trophozoite–stage parasites, but did specifically recognize an antigen expressed by late schizont–infected RBCs (Fig. 3, A and B). To determine whether antibodies to PfSEA-1 could access PfSEA-1 in vivo, we used a live cell–labeling technique. PfSEA-1 colocalized with glycophorin A in nonpermeabilized, unfixed schizont-infected RBCs (Fig. 3C). We confirmed the stage-specific expression and localization of PfSEA-1 using antibodies to the HA tag in D10-PfSEA1-DD parasites, in which PfSEA-1 is fused with an HA tag (fig. S7).

The accessibility of antibodies to PfSEA-1 in living parasites was further evaluated by immuno–electron microscopy (Fig. 3D and fig. S8). When the same live cell–labeling technique was used, PfSEA-1 localized to the schizont/parasitophorous vacuole membrane, Maurer's clefts, and the inner leaflet of the RBC membrane, whereas glycophorin A was confined to the outer leaflet of the RBC membrane. This pattern of staining was observed in the majority of late schizont–infected RBCs examined. The close juxtaposition of these structures in late schizont–infected RBCs with the RBC outer membrane explains the apparent colocalization of PfSEA-1 with glycophorin A observed by confocal microscopy. The accessibility of antibodies to PfSEA-1 in nonpermeabilized, unfixed schizont–infected RBCs is consistent with the known permeability of parasitized RBCs to macromolecules, including antibodies, at the later stages of schizogony (*18*–*20*).

Anti–PfSEA-1 Mediates Schizont Arrest of Parasites in Vitro

The localization of PfSEA-1 was not consistent with a role in RBC invasion; rather, it suggested a role in parasite egress from RBCs. To determine the mechanism of growth inhibition, we performed schizont arrest assays using anti–rPfSEA-1A prepared by either DNA or recombinant protein immunization, as well as mAb directed against rPfSEA-1A (Fig. 4). Parasites were synchronized to the ring stage at high (3.5%) parasite density, cultured to obtain early schizonts, and then incubated with anti–rPfSEA-1A or controls for 12 hours, followed by enumeration of the remaining schizont-stage parasites. Under these conditions, the majority of schizont-infected RBCs should rupture, releasing merozoites to invade new RBCs and develop into ring-stage parasites. Anti–rPfSEA-1A generated by DNA plasmid– (Fig. 4, A to C) or recombinant protein– (Fig. 4, D and E, and fig. S9) based immunization, as well as mAb anti–rPfSEA-1A (Fig. 4F) inhibited schizont egress in a dose-dependent manner (Fig. 4G), resulting in 4.3- to 6.8-fold higher proportions of schizonts across three parasite strains as compared with controls (all $P < 0.009$). In addition, purified human polyclonal antibodies to PfSEA-1 significantly inhibited schizont egress (fig. S6C).

Vaccination with PbSEA-1 Protects Mice from *P. berghei* ANKA Challenge

To evaluate the protective efficacy of vaccination with SEA-1 in vivo, we selected the *Plasmodium berghei* ANKA strain model, because of its aggressive parasite growth rate, extreme lethality in mice, and the failure of known vaccine candidates [such as PbAMA-1 and PbMSP-1 (*21*)] to afford protection. We cloned the *P. berghei* ANKA strain ortholog of rPfSEA-1A (nt 2173 to 3000, 47% similar and 34% identical amino acid sequence as compared with rPfSEA-1A) into the expression plasmid pET30 and expressed and purified rPbSEA-1A (amino acids 725 to 1000) from *E. coli* (Fig. 5A). We conducted five (four active vaccination with rPbSEA-1A and one passive transfer of antibodies to PbSEA-1A) trials in mice with *P. berghei* ANKA challenge. After vaccination, mice generated robust anti–rPbSEA-1A immunoglobulin G (IgG) responses in each trial (Fig. 5B and fig. S10). In trial 1, BALB/c mice vaccinated intraperitoneally (ip) with TiterMax and challenged ip with 10^6 *P. berghei* ANKA–infected RBCs (iRBCs) had 2.25-fold higher parasitemia on day 7 after challenge, as compared with mice vaccinated with rPbSEA-1A in TiterMax

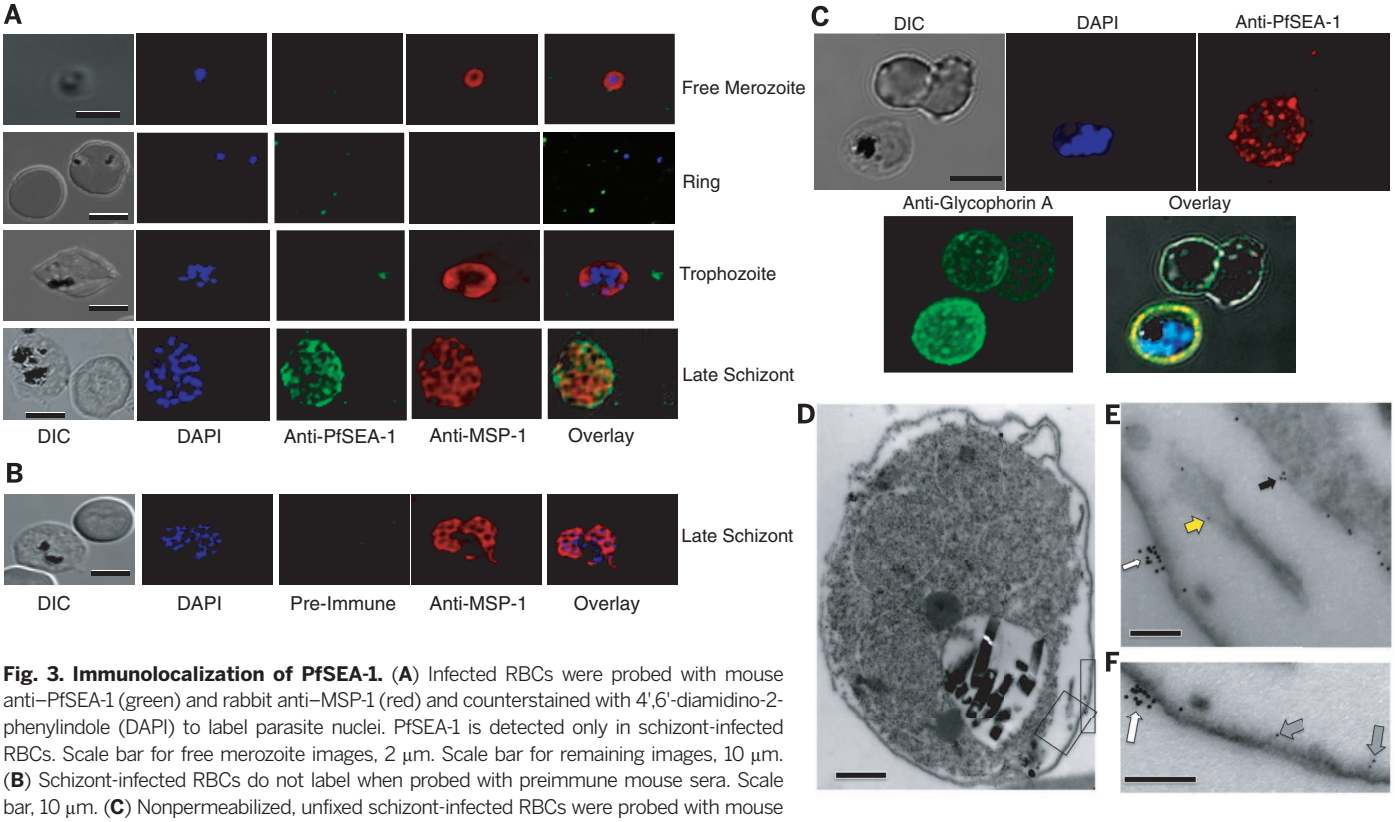

Fig. 3. Immunolocalization of PfSEA-1. (**A**) Infected RBCs were probed with mouse anti–PfSEA-1 (green) and rabbit anti–MSP-1 (red) and counterstained with 4',6'-diamidino-2-phenylindole (DAPI) to label parasite nuclei. PfSEA-1 is detected only in schizont-infected RBCs. Scale bar for free merozoite images, 2 μm. Scale bar for remaining images, 10 μm. (**B**) Schizont-infected RBCs do not label when probed with preimmune mouse sera. Scale bar, 10 μm. (**C**) Nonpermeabilized, unfixed schizont-infected RBCs were probed with mouse anti–PfSEA-1 (red) and rabbit anti–glycophorin A (green) and counterstained with DAPI to label parasite nuclei. PfSEA-1 colocalized with glycophorin A to the surface of schizont-infected RBCs. Scale bar, 5 μm. (**D** to **F**) Nonpermeabilized, unfixed schizont-infected RBCs were probed with mouse anti–PfSEA-1 (5-nm gold particles) and rabbit anti–glycophorin A (10-nm gold particles). PfSEA-1 localized to the schizont/parasitophorous vacuole membrane (black arrow), Maurer's clefts (yellow arrow), and the inner leaflet of the RBC membrane (gray arrow), whereas glycophorin A was confined to the outer leaflet of the RBC membrane (white arrow). Scale bar in (D), 0.5 μm. Scale bars in (E) and (F), 0.1 μm.

(Mann-Whitney U test, $P = 0.0002$, Fig. 5C). All control mice were killed on day 7 because of high parasitemia and associated illness, in accordance with our animal protocol Center for International Health Research, Rhode Island Hospital (CIHR). In trial 2, C57BL/6 mice vaccinated subcutaneously (sc) with TiterMax and challenged with 200 *P. berghei* ANKA sporozoites intravenously (iv) had 1.52-fold higher parasitemia on day 7 after challenge, as compared with mice vaccinated with rPbSEA-1A in TiterMax (Mann-Whitney U test, $P = 0.002$, Fig. 5D). All mice were killed on day 8 in accordance with our animal protocol (National Institutes of Health). In trial 3, BALB/c mice vaccinated ip with TiterMax and challenged ip with 10^4 *P. berghei* ANKA iRBC had 3.05-fold higher parasitemia on day 7 after challenge, as compared with mice vaccinated with rPbSEA-1A in TiterMax (Mann-Whitney U test, $P = 0.001$, Fig. 5E). All control mice were killed on day 8 because of high parasitemia and associated illness, in accordance with our animal protocol (CIHR). Trials 4 (active vaccination with rPbSEA-1A) and 5 (passive transfer of antibodies to PbSEA-1A) were conducted under a modified animal protocol (CIHR) that allowed the collection of survival outcomes. In trial 4, BALB/c mice vaccinated ip with TiterMax and challenged ip with 10^4 *P. berghei* ANKA iRBC had 3.9-fold as high parasitemia on day 7 after challenge, as compared with mice vaccinated with rPbSEA-1A in TiterMax (Mann-Whitney U test, $P = 0.0009$, Fig. 5F). The median survival of rPbSEA-1A–vaccinated mice was 1.8-fold longer than that of mice vaccinated with TiterMax alone (log-rank test, $P < 0.0001$, Fig. 5G).

To evaluate the role of humoral anti–SEA-1 responses in mediating protection, we conducted passive transfer experiments, followed by *P. berghei* ANKA challenge. In trial 5, BALB/c mice passively transferred with control mouse sera and challenged ip with 10^4 *P. berghei* ANKA iRBC had 2.7-fold higher parasitemia on day 7 after challenge, as compared to mice passively transferred with anti–PbSEA-1A (Mann-Whitney test, $P = 0.009$, Fig. 5H). The median survival of mice treated with anti–rPbSEA-1A was 2.0-fold longer than that of mice treated with control sera (log-rank test, $P < 0.0001$, Fig. 5I).

Our active vaccine studies included two routes of administration (sc and ip), two stages of challenge (sporozoite and iRBC), two doses of iRBC challenge (10^4 and 10^6 iRBC per mouse), two vaccination schedules, two mouse strains (BALB/c and C57BL/6), two methods of enumeration (microscopy and flow cytometry), and two performance sites (CIHR and NIH). In all experiments, rPbSEA-1A generated significant protection. These results represent the first example of significantly reduced parasitemia and delayed mortality after vaccination with a blood-stage antigen in *P. berghei* ANKA (*21*).

Human Antibody Responses to PfSEA-1 *Tanzanian Birth Cohort*

To evaluate the impact of naturally acquired antibodies to PfSEA-1 on clinical malaria, we measured antibody to PfSEA-1 IgG levels using a fluorescent bead–based assay in our birth cohort and related these levels to subsequent malaria outcomes. We measured levels of antibody to PfSEA-1 IgG in available plasma obtained at scheduled, nonsick visits between 1.5 and

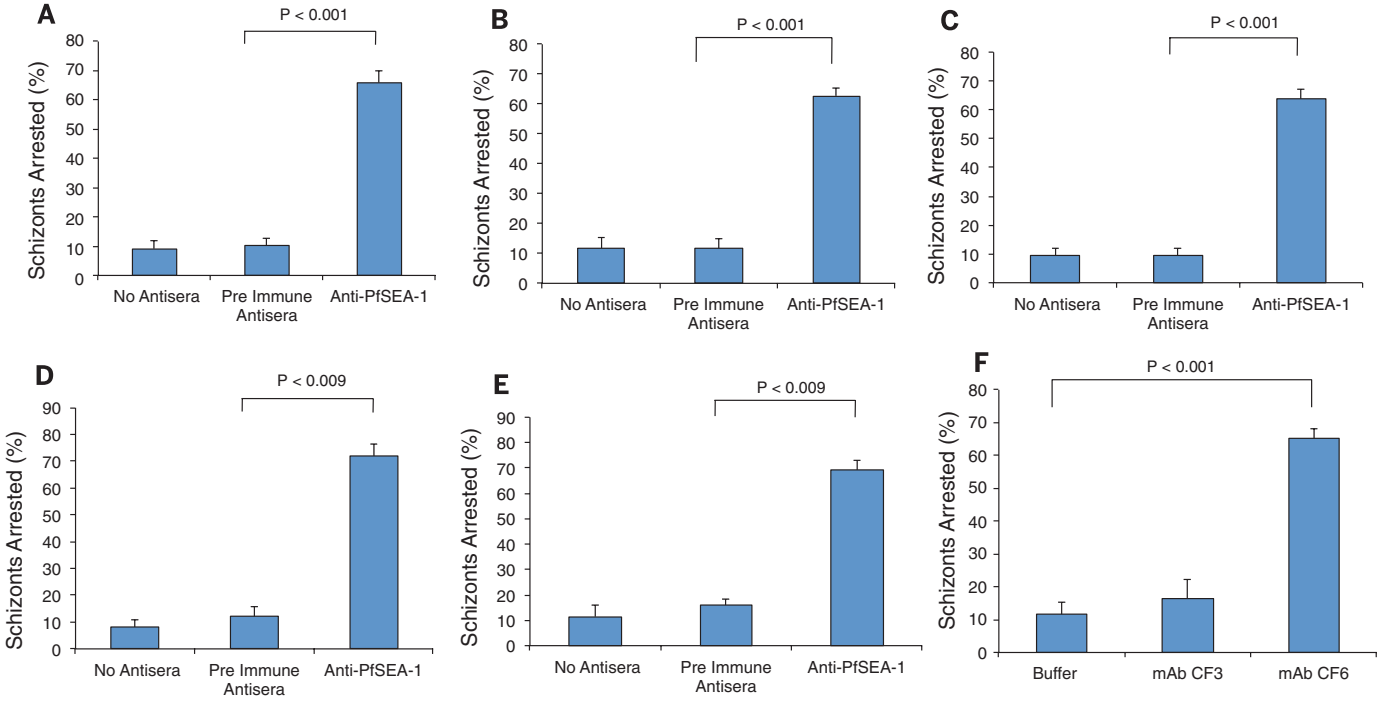

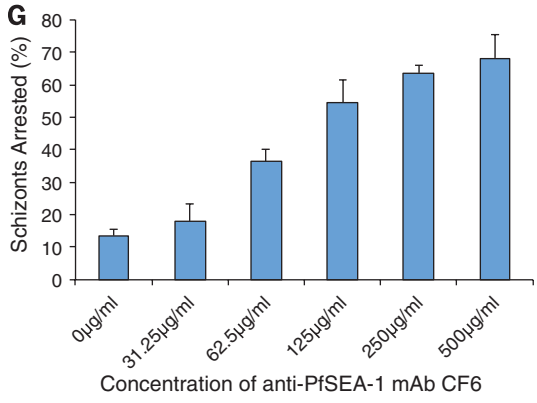

Fig. 4. Antibodies to PfSEA-1 inhibit schizont egress. Antibodies to PfSEA-1 generated by DNA (**A** to **C**) and recombinant protein (**D** and **E**) immunization, as well as mAb to rPfSEA-1A (**F** and **G**), inhibit schizont egress for three parasite strains in vitro. Early schizont stage 3D7 [(A) and (D)], W2 [(B) and (E)], and D10 (C) parasites were incubated in the presence of mouse anti–PfSEA-1 (1:10 dilution). Negative controls included no mouse sera and preimmune mouse sera (1:10 dilution). In (F), 3D7 parasites were incubated in the presence of mAbs to PfSEA-1 CF3 or CF6 (at 250 µg/ml) or buffer. In (G), 3D7 parasites were incubated in the presence of increasing concentrations of mAb to PfSEA-1 CF6 or buffer. Schizonts were counted 12 hours after treatment, and the percent of initial schizonts arrested was calculated. Bars represent the mean of five independent replicates, with each replicate performed in triplicate. Error bars represent SEMs. Comparisons between pre- and postimmune mouse sera and between buffer and mAb-treated cultures by a nonparametric Mann-Whitney U test are indicated. All panels are representative of three independent experiments.

3.5 years of life, encompassing 687 antibody measures on 453 children. The average time interval between each antibody measurement and either a subsequent antibody determination or completion of the study was 39 weeks. For each antibody measurement, the analysis interval for malaria outcomes extended from the time of the antibody measurement until the child had a subsequent antibody determination or completed the study.

Antibodies to PfSEA-1 were detectable in 6.0% of these samples, and children were followed for a total of 25,494 child-weeks of observation. We used Cox proportional hazards models to evaluate the relationship between

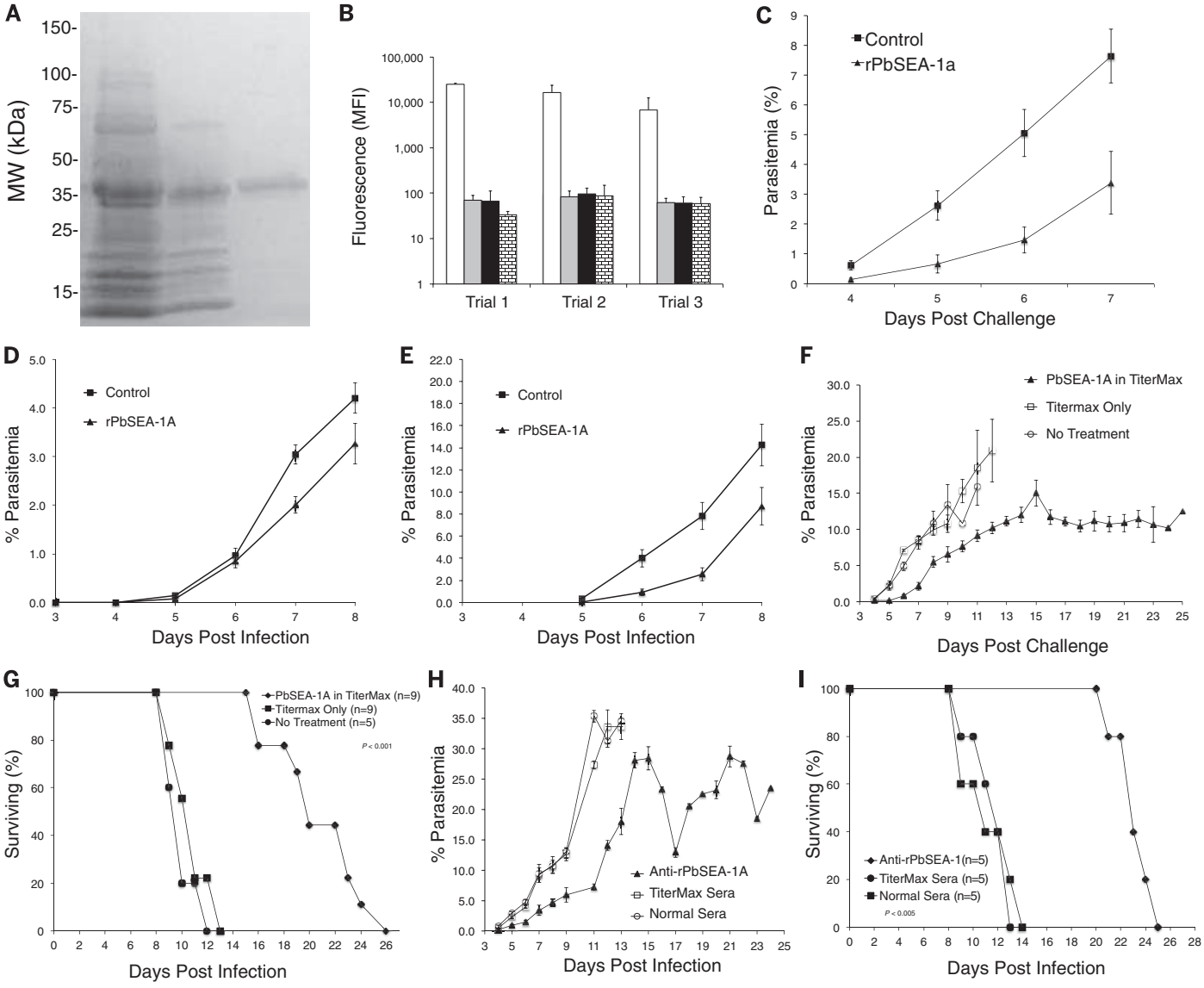

Fig. 5. Vaccination with rPbSEA-1A protects mice from challenge with *P. berghei* ANKA. (**A**) Expression and purification of rPbSEA-1A from *E. coli* soluble lysates. Lane 1, nickel chelate chromatography of soluble *E. coli* lysate; lane 2, hydrophobic interaction chromatography of lane 1; lane 3, anion exchange chromatography of lane 2. (**B**) Antibody response of mice vaccinated with rPbSEA-1A in three vaccine trials. After vaccination, mice generated robust anti–rPbSEA-1A IgG responses in each trial. Bars represent mean fluorescence; error bars represent SEMs. White bars represent anti–rPbSEA-1A IgG responses in mice immunized with rPbSEA-1A, gray bars represent anti-BSA IgG responses in mice immunized with rPbSEA-1A, black bars represent anti–rPbSEA-1A IgG responses in mice immunized with adjuvant alone, and bricked bars represent anti-BSA IgG responses in mice immunized with adjuvant alone. (**C**) Vaccine trial 1: BALB/c mice vaccinated ip with TiterMax (n = 11) and challenged ip with 10^6 *P. berghei* ANKA–infected RBCs had 2.25-fold higher parasitemia on day 7 after challenge (P = 0.0002) as compared to mice vaccinated with rPbSEA-1A (n = 10). (**D**) Vaccine trial 2: C57BL/6 mice vaccinated sc with TiterMax (n = 10) and challenged with 200 *P. berghei* ANKA sporozoites iv had 1.52-fold higher parasitemia on day 7 after challenge (P = 0.002) as compared to mice vaccinated with rPbSEA-1A (n = 10). (**E**) Vaccine trial 3: BALB/c mice vaccinated ip with TiterMax (n = 10) and challenged ip with 10^4 *P. berghei* ANKA–infected RBCs had 3.05-fold higher parasitemia on day 7 after challenge (P = 0.001) as compared to mice vaccinated with rPbSEA-1A (n = 10). (**F** and **G**) Vaccine trial 4: BALB/c mice vaccinated ip with TiterMax (n = 9) and challenged ip with 10^4 *P. berghei* ANKA–infected RBCs had 3.9-fold higher parasitemia on day 7 after challenge (P = 0.0009) as compared to mice vaccinated with rPbSEA-1A in TiterMax. The median survival of rPbSEA-1A vaccinated mice was 1.8-fold longer (P < 0.0001) as compared to that of adjuvant-only control mice (n = 9). (**H** and **I**) Vaccine trial 5: Antisera (rPbSEA-1A or adjuvant alone) or normal mouse sera were passively transferred (0.5 ml, ip) into naïve BALB/c mice (n = 5 mice per group) on day −1 and day +1. On day 0, mice were challenged ip with 10^4 *P. berghei* ANKA–infected RBCs. Control mice had 2.7-fold higher parasitemia on day 7 after challenge (P = 0.009), compared to anti-rPbSEA-1A treated mice. The median survival of rPbSEA-1A vaccinated mice was 2.0-fold longer than that of controls (P < 0.0001).

time-varying levels of antibody to PfSEA-1 (log-transformed) and malaria outcomes. Increasing levels of antibody to PfSEA-1 were associated with significantly decreased risk of severe malaria [HR = 0.669, 95% confidence interval (CI) [0.495, 0.905], P = 0.0092], and these results were essentially identical after adjusting for hemoglobin phenotype (HR = 0.663, 95% CI [0.489, 0.897], P = 0.0078). It was surprising that severe malaria did not occur during periods after children had detectable levels of antibody to PfSEA-1 (0 cases per 1688 child-weeks with detectable antibody to PfSEA-1 versus 45 cases per 23,806 child-weeks with undetectable antibody to PfSEA-1) (Fig. 6A).

To place the PfSEA-1 antibody results in context with other known malarial vaccine candidates, we performed multiplexed bead-based antibody analyses using plasma collected at 2 years of age from n = 225 available samples in our birth cohort. Using this multiplexed platform, we measured IgG antibody levels to MSP-1-19 (3D7 variant), MSP-3 (amino acids 99 to 265), LSA-N (amino acids 28 to 150), LSA-C (amino acids 1630 to 1909), and RAMA-E (amino acids 759 to 840). IgG antibody responses to these well-accepted vaccine candidates were not related to the risk of severe malaria when the same statistical analyses employed for PfSEA-1 were used in these available samples (all P = NS, see supplementary text).

Together, these results demonstrate that antibodies that specifically block schizont egress can predict resistance to severe malaria in humans and provide compelling evidence that PfSEA-1 represents a critical addition to the limited pool of candidate antigens currently being explored for their vaccine potential.

Kenyan Cohort

To further extend the generalizability of our human immunoepidemiologic results, we measured anti–PfSEA-1 IgG responses in an entirely distinct cohort of Kenyan adolescents and young adults. We performed a secondary analysis with data and serum samples that were collected from a cohort of Kenyan males as part of a treatment-reinfection study (*7*, *12*, *22*).

Volunteers were residents of subsistence farming, *P. falciparum*–endemic villages in western Kenya, north of Lake Victoria. The entomological inoculation rate in this area exceeded 300 infectious bites per person per year (*23*), and bed nets had not been introduced into the community. Males (n = 138) aged 12 to 35 years were entered into the study at the beginning of the high transmission season in April 1997. Detectable parasitemia was eradicated by the use of quinine sulfate (10 mg per kilogram of body weight twice daily for 3 days) and doxycycline (100 mg twice daily for 7 days), and individuals were followed with weekly blood smears for 18 weeks. Serum was collected 2 weeks after treatment and stored at −80°C. In this age group, clinical or severe malaria is very uncommon.

In generalized estimating equation (GEE) repeated-measures models, individuals with detectable IgG antibodies to rPfSEA-1A (n = 77 individuals who contributed 1154 weeks of follow-up blood smears) had 50% lower parasite densities over 18 weeks of follow-up than did individuals with no detectable IgG antibodies to rPfSEA-1A (n = 61 individuals who contributed 940 weeks of follow-up blood smears), after adjusting for age, week of follow-up, exposure to *Anopheles* mosquitoes, and hemoglobin phenotype (95% CI [3, 97], P < 0.04, Fig. 6B). We measured IgG antibody levels to MSP-3 (amino acids 99 to 265), MSP-7 (amino acids 117 to 248), LSA-N (amino acids 28 to 150), LSA-C (amino acids 1630 to 1909), and RAMA-E (amino acids 759 to 840) in these same samples. IgG antibody responses to these well-accepted vaccine candidates did not predict resistance to parasitemia in these samples when the same statistical analyses employed for PfSEA-1 were used (fig. S11, all P = NS).

Although residual confounding by unmeasured factors cannot be completely excluded, together with the data from the Tanzanian birth cohort, these data generalize and underscore the relation between anti–PfSEA-1 IgG responses and resistance to parasitemia and severe falciparum malaria in humans.

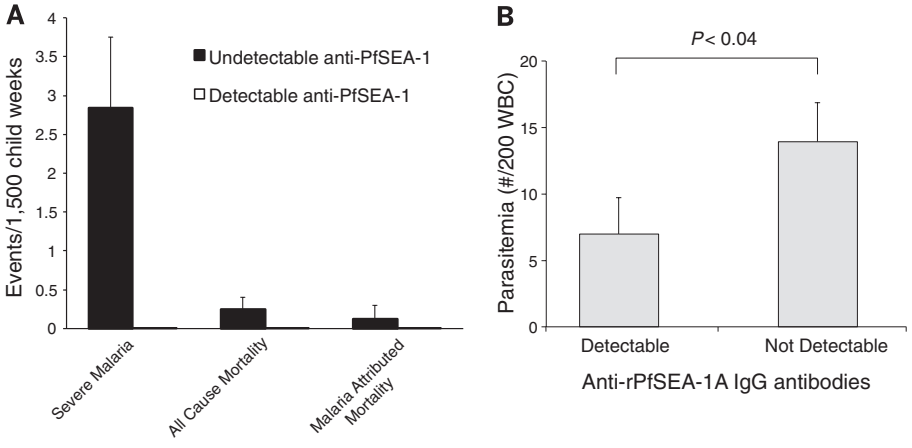

Fig. 6. Antibodies to rPfSEA-1A predict reduced malaria severity and parasitemia. (**A**) Incidence of severe malaria and death in Tanzanian children aged 1.5 to 3.5 years during intervals with detectable and undetectable antibodies to PfSEA-1 (1688 and 23,806 weeks, respectively). No cases of severe malaria or death occurred during intervals with detectable antibodies to rPfSEA-1A. Error bars represent 95% CI, adjusted for repeated measures. (**B**) IgG antibodies to rPfSEA-1A predict decreased *P. falciparum* parasitemia. We enrolled n = 138 Kenyan males aged 12 to 35 years at the start of a high-transmission season, treated them with quinine and doxycycline, and followed them for 18 weeks with weekly blood smears. We collected serum 2 weeks after treatment and measured IgG antibody levels to rPfSEA-1A. In GEE repeated-measures models, individuals with detectable IgG antibodies to rPfSEA-1A had 50% lower parasite densities over 18 weeks of followup as compared to individuals with no detectable IgG antibodies to rPfSEA-1A, after adjusting for potential confounders (P < 0.04). Columns depict least-square mean parasitemia; error bars depict SEM.

Summary and Conclusions

Falciparum malaria remains a leading cause of childhood mortality, and vaccines are urgently needed to attenuate this public health threat. We report the rational identification of novel vaccine candidates by identifying parasite proteins recognized by antibodies expressed by resistant, but not susceptible, children. We identified two previously unknown hypothetical genes as well as MSP-7, a known vaccine candidate (*9*–*12*). We have extensively characterized PfSEA-1, which localizes to the schizont/parasitophorous vacuole membrane, Maurer's clefts, and the inner leaflet of the RBC membrane in schizont-infected RBCs. PfSEA-1 is accessible to antibodies during late schizogeny and displays minimal sequence variation in the immunorelevant region identified by our differential screening experiments (amino acids 810 to 1083). Antibodies to PfSEA-1 significantly attenuate parasite growth by arresting schizont egress from infected RBCs. Concordant with these results, genetically destabilizing PfSEA-1 results in a dramatic 80% inhibition of parasite growth.

In five challenge experiments, rPbSEA-1A or antibodies to PbSEA-1A conferred marked protection against a lethal *P. berghei* ANKA challenge as evidenced by up to a 75% reduction in parasitemia 7 days after challenge. In all five experiments, by day 7 to 8 after challenge, control mice had high parasitemia with associated morbidity, whereas none of the vaccinated mice had high parasitemia or overt morbidity. In experiments with long-term follow-up, both active immunization with rPbSEA-1 and passive transfer of antisera to PbSEA-1 significantly reduced parasitemia and delayed mortality. We report protection from *P. berghei* ANKA by vaccination with a blood-stage antigen, and these data support our ongoing efforts to evaluate PfSEA-1 in the *Aotus* model of *P. falciparum*.

In our Tanzanian birth cohort, antibodies to PfSEA-1 were associated with significant protection from severe malaria, with no cases occurring

while children had detectable antibodies to PfSEA-1. These data suggest that anti–PfSEA-1 responses could augment responses to other targets, such as PfEMP-1, that may protect against severe malaria (*24*). Under conditions of natural exposure, only 6% of 1.5- to 3.5-year-old children in our cohort had detectable antibodies to PfSEA-1. This low natural prevalence suggests that adjuvanted vaccination with PfSEA-1 could have a marked impact on reducing severe malaria in young children.

In a second longitudinal Kenyan cohort, anti–PfSEA-1 antibodies were associated with significant protection against parasitemia in adolescents and young adults. Individuals with detectable IgG anti–rPfSEA-1A antibodies had 50% lower parasite densities over 18 weeks of follow-up compared with individuals with no detectable IgG anti-rPfSEA-1A antibodies. It was noteworthy that the prevalence of detectable anti–rPfSEA-1A antibodies in this age group (56%) was substantially higher than in our birth cohort, which suggests that natural exposure boosts anti–PfSEA-1 antibody levels.

Together, our data validate our field-to-lab-to-field-based strategy for the rational identification of vaccine candidates and support PfSEA-1 as a candidate for pediatric falciparum malaria. By blocking schizont egress, PfSEA-1 may synergize with other vaccines targeting hepatocyte (*25*) and RBC invasion (*26*).

REFERENCES AND NOTES

1. C. J. Murray *et al.*, *Lancet* **379**, 413–431 (2012).
2. WHO, *The World Malaria Report* (WHO, Switzerland, 2012); www.who.int/malaria/publications/world_malaria_report_2012/en/index.html.
3. S. Okie, *N. Engl. J. Med.* **353**, 1877–1881 (2005).
4. WHO, Malaria Vaccine Rainbow Tables (2012); www.who.int/vaccine_research/links/Rainbow/en/index.html.
5. A. N. Hodder, P. E. Crewther, R. F. Anders, *Infect. Immun.* **69**, 3286–3294 (2001).
6. A. Sabchareon *et al.*, *Am. J. Trop. Med. Hyg.* **45**, 297–308 (1991).
7. J. D. Kurtis, D. E. Lanar, M. Opollo, P. E. Duffy, *Infect. Immun.* **67**, 3424–3429 (1999).
8. T. K. Mutabingwa *et al.*, *PLOS Med.* **2**, e407 (2005).
9. R. Spaccapelo *et al.*, *Sci. Rep.* **1**, 39 (2011).
10. N. D. Gómez *et al.*, *PLOS ONE* **6**, e25477 (2011).
11. M. Kadekoppala, R. A. O'Donnell, M. Grainger, B. S. Crabb, A. A. Holder, *Eukaryot. Cell* **7**, 2123–2132 (2008).
12. C. P. Nixon *et al.*, *J. Infect. Dis.* **192**, 861–869 (2005).
13. M. Treeck, J. L. Sanders, J. E. Elias, J. C. Boothroyd, *Cell Host Microbe* **10**, 410–419 (2011).
14. M. Manske *et al.*, *Nature* **487**, 375–379 (2012).
15. J. D. Dvorin *et al.*, *Science* **328**, 910–912 (2010).
16. A. Farrell *et al.*, *Science* **335**, 218–221 (2012).
17. M. J. Blackman, H. G. Heidrich, S. Donachie, J. S. McBride, A. A. Holder, *J. Exp. Med.* **172**, 379–382 (1990).
18. E. S. Bergmann-Leitner, E. H. Duncan, E. Angov, *Malar. J.* **8**, 183 (2009).
19. N. Ahlborg *et al.*, *Exp. Parasitol.* **82**, 155–163 (1996).
20. I. D. Goodyer, B. Pouvelle, T. G. Schneider, D. P. Trelka, T. F. Taraschi, *Mol. Biochem. Parasitol.* **87**, 13–28 (1997).
21. S. Yoshida *et al.*, *PLOS ONE* **5**, e13727 (2010).
22. J. D. Kurtis, R. Mtalib, F. K. Onyango, P. E. Duffy, *Infect. Immun.* **69**, 123–128 (2001).
23. J. C. Beier *et al.*, *Am. J. Trop. Med. Hyg.* **50**, 529–536 (1994).
24. P. C. Bull *et al.*, *J. Infect. Dis.* **192**, 1119–1126 (2005).
25. RTS,S Clinical Trials Partnership, *N. Engl. J. Med.* **365**, 1863–1875 (2011).
26. C. Crosnier *et al.*, *Nature* **480**, 534–537 (2011).

ACKNOWLEDGMENTS

The authors thank the Mother Offspring Malaria Study project staff for their efforts in collecting clinical data, processing samples, and interpreting malaria blood smears, as well as the study participants and their families. Ethical clearance was obtained from the institutitional review boards of the Seattle Biomedical Research Institute and Rhode Island Hospital; the Medical Research Coordinating Committee of the National Institute for Medical Research, Tanzania; and the Kenyan Medical Research Institute. We thank A. Muehlenbachs for assistance in interpreting the electron microscopy images, B. Morrison for assistance with data management, and D. Lanar for the LSA proteins. This work was supported by grants from the U.S. National Institutes of Health (NIH) (grant R01-AI52059) and the Bill & Melinda Gates Foundation (grant 1364) to P.E.D., the Intramural Research Program of the National Institute of Allergy and Infectious Diseases–NIH, and grants from NIH (grant R01-AI076353) and an internal Lifespan Hospital System Research Pilot Award Grant to J.D.K., and grants from NIH to J.D.D. (R01-AI102907 and DP2-AI112219). C.E.N. (grant T32-DA013911) and I.C.M. (grant 1K08AI100997-01A1) were supported by NIH. We also acknowledge research core services provided by the Rhode Island Hospital imaging core (G. Hovanesian) and core services supported by Lifespan/Tufts/Brown Center for Aids Research (P30AI042853) and Center for Biomedical Research Excellence (P20GM103421). The DNA sequence for PfSEA-1 is available in PlasmoDB (www.Plasmodb.org) as ID no. PF3D7_1021800. The work presented in this manuscript has been submitted in partial support of patent application PCT/US12/67404 filed with the U.S. Patent Office. J.D.K., J.F.F., M.F., and P.E.D. designed the study; J.D.K., D.K.R., J.F.F., M.F., and P.E.D. drafted the manuscript; M.F. and P.E.D. conducted the field-based sample and epidemiologic data collection; C.P.N. conducted the differential screening; D.K.R, L.P., A.L., C.E.N., and L.C. performed the in vitro growth assays; D.K.R. and G.J. performed the immunolocalization; D.K.R. performed the gene knockout studies; C.G.D., E.A.M., S.A., and J.D.D. performed the conditional gene knockdown studies; I.C.M. performed the single-nucleotide polymorphism detection; S.P.-T., L.C., and H.-W.W. performed the antibody detection assays; S.P.-T. expressed and purified rPfSEA-1A and rPbSEA-1A; D.K.R., C.E.N., and S.C. performed the vaccination studies; J.F.F., J.D.K., and S.E.H. performed the statistical analyses; and J.D.K., J.F.F., M.F., and P.E.D. supervised the study. The authors declare no competing financial interests.

SUPPLEMENTARY MATERIALS

www.sciencemag.org/content/334/6186/871/suppl/DC1
Materials and Methods
Supplementary Text
Tables S1 and S2
Figs. S1 to S11
References (*27*–*41*)

30 October 2013; accepted 25 April 2014
10.1126/science.1254417

DEEP EARTH

Disproportionation of $(Mg,Fe)SiO_3$ perovskite in Earth's deep lower mantle

Li Zhang,[1,2]* Yue Meng,[3] Wenge Yang,[1,4] Lin Wang,[1,4] Wendy L. Mao,[5,6] Qiao-Shi Zeng,[5] Jong Seok Jeong,[7] Andrew J. Wagner,[7] K. Andre Mkhoyan,[7] Wenjun Liu,[8] Ruqing Xu,[8] Ho-kwang Mao[1,2]

The mineralogical constitution of the Earth's mantle dictates the geophysical and geochemical properties of this region. Previous models of a perovskite-dominant lower mantle have been built on the assumption that the entire lower mantle down to the top of the D″ layer contains ferromagnesian silicate [$(Mg,Fe)SiO_3$] with nominally 10 mole percent Fe. On the basis of experiments in laser-heated diamond anvil cells, at pressures of 95 to 101 gigapascals and temperatures of 2200 to 2400 kelvin, we found that such perovskite is unstable; it loses its Fe and disproportionates to a nearly Fe-free $MgSiO_3$ perovskite phase and an Fe-rich phase with a hexagonal structure. This observation has implications for enigmatic seismic features beyond ~2000 kilometers depth and suggests that the lower mantle may contain previously unidentified major phases.

The conventional view of materials in Earth's lower mantle, which comprises the largest fraction of our planet (>55% by volume), has evolved greatly in the past 10 years. High-pressure-temperature (*P-T*) experiments of the past century suggested that the predominant phase was ferromagnesian silicate [$(Mg,Fe)SiO_3$] with the orthorhombic perovskite (pv) structure, unchanging over the enormous *P-T* range from the bottom of the transition zone at 670 km depth (24 GPa) to the core-mantle boundary (CMB) at 2900 km (136 GPa). However, laser-heated diamond anvil cell (DAC) technology coupled with x-ray spectroscopy (XRS) and x-ray diffraction (XRD) probes have led to two key discoveries: namely, the phase transition of $(Mg,Fe)SiO_3$ pv to the post-perovskite (ppv) structure (*1*–*3*) near the D″ layer of the lower mantle, and the pressure-induced spin-pairing of the *3d* electrons in Fe (*4*–*6*)

[1]Center for High Pressure Science and Technology Advanced Research (HPSTAR), Shanghai 201203, China. [2]Geophysical Laboratory, Carnegie Institution of Washington (CIW), Washington, DC 20015, USA. [3]High Pressure Collaborative Access Team (HPCAT), Geophysical Laboratory, CIW, Argonne, IL 60439, USA. [4]High Pressure Synergetic Consortium (HPSynC), Geophysical Laboratory, CIW, Argonne, IL 60439, USA. [5]Geological and Environmental Sciences, Stanford University, Stanford, CA 94305, USA. [6]Photon Science, SLAC National Accelerator Laboratory, Menlo Park, CA 94025, USA. [7]Department of Chemical Engineering and Materials Science, University of Minnesota, Minneapolis, MN 55455 USA. [8]Advanced Photon Source, Argonne National Laboratory, Argonne, IL 60439, USA.
***Corresponding author. E-mail: zhangli@hpstar.ac.cn**